

Numerical study of droplet evaporation in coupled high-temperature and electrostatic fields

Ziwen Zuo, Junfeng Wang, Yuanping Huo and Yajun Fan

Abstract

The evaporation of a sessile water droplet under the coupled electrostatic and high-temperature fields is studied numerically. The leaky dielectric model and boiling point evaporation model are used for calculating the electric force and heat mass transfer. The free surface is captured using the volume of fluid method accounting for the variable surface tension and the transition of physical properties across the interface. The flow behaviors and temperature evolutions in different applied fields are predicted. It shows that in the coupled fields, the external electrostatic field restrains the flow inside the droplet and keeps a steady circulation. The flow velocity is reduced due to the interaction between electric body force and the force caused by temperature gradient. The heat transfer from air into the droplet is reduced by the lower flow velocity. The evaporation rate of the droplet in the high-temperature field is decreased.

Keywords

High temperature, evaporation, electrostatic field, droplet

Date received: 23 August 2014; accepted: 8 January 2015

Academic Editor: Sang-Wook Kang

Introduction

The phenomenon of droplet evaporation in high-temperature condition is not too far away from our daily life such as spilled water on the induction cooker. It is even more in industries from jet quenching to spray smoke dust control. Due to high-temperature operation condition, the evaporation behaviors of the water droplet are more complex. Therefore, the relevant problems become an interesting study direction. Renksizbulut and Yuen^{1,2} studied the droplet evaporation in a high-temperature stream by both experimental and numerical methods. They provided a non-dimensional number correlation for evaporation to determine whether the evaporation rate reduced. Harpole³ presented a stagnation-point solution to investigate the evaporation properties with more comprehensive affecting factors: blowing variable fluid properties, interdiffusion, and radiation. Beyond the

pure academic studies, explores with industrial background seem more attractive due to the economic benefits. For many of the simulation models, the calculating time is too long to be accepted. Abramzon and Sirignano⁴ developed a simple but sufficiently accurate model for spray combustion calculations. The radiation absorption becomes an important energy exchange when the work temperature is very high. Tseng and Viskanta⁵ numerically verified this factor.

Under the influence of an applied electrostatic field, the sessile droplet experiences specific behaviors.

School of Energy and Power Engineering, Jiangsu University, Zhenjiang, China

Corresponding author:

Junfeng Wang, School of Energy and Power Engineering, Jiangsu University, 301 Xuefu Road, Zhenjiang 086-212013, China.
Email: wangjunfeng@ujs.edu.cn



Creative Commons CC-BY: This article is distributed under the terms of the Creative Commons Attribution 3.0 License (<http://www.creativecommons.org/licenses/by/3.0/>) which permits any use, reproduction and distribution of the work without further permission provided the original work is attributed as specified on the SAGE and Open Access pages (<http://www.uk.sagepub.com/aboutus/openaccess.htm>).

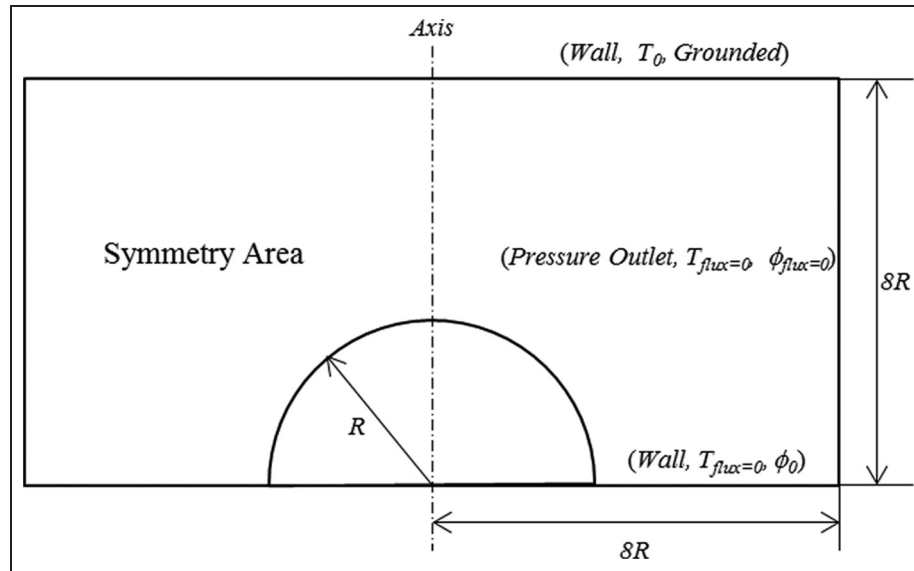


Figure 1. Schematic of the axisymmetric model.

Together with evaporation process, the characteristics will become more complex and valuable to explore. Hashinaga et al.⁶ studied the evaporation of water under the electric field. They found that whatever the alternating current, the direct currents could enhance the evaporation rate of the water liquid. Gamero-Castano⁷ found that within the evaporated mass, the emitted ion current is a very steep function of the electric field. Balachandran et al.⁸ removed the smoke particles by using the charged water spray. The results showed that the removable efficiency of smoke particles for the charged system is significantly higher than that of the uncharged system. Bateni et al.⁹ developed a new axisymmetric drop shape analysis for electric fields (ADSA-EF) and finite element method-based numerical scheme to investigate the correlation between the surface tension of conducting drop and electric field by considering the gravity. Chen et al.¹⁰ experimentally studied the initial spreading of a liquid drop under the electrostatic field. They found that the spreading dynamics was relative with electrolyte concentration and a simple mathematical model was proposed. Vancauwenbergh et al.¹¹ systematically reviewed the evaporation of sessile droplet under the influence of the electric field. The change in contact angle, the shape, and the evaporation rate of the droplet were mainly discussed. The article pointed out that the aim of such studies was to accurately control the evaporation rate of the droplet through the electrical way. It should be noted that all these investigations are carried out at the room temperature. In practice, the work condition is not always as low as this. For instance, the smokes from power plants are very high. The behaviors that were

presented from charged droplets in high-temperature condition are seldom reported in the literatures. This article is based on boiling point evaporation model and leaky dielectric model,¹² using volume of fluid (VOF) free surface capture method¹³ to numerically investigate the characteristics of the evaporating droplet under high-temperature condition subjected to the electrostatic field. The heat transfer of the droplet under the single high-temperature field and the coupled electrostatic field is compared. The influences of three applied conditions, high-temperature, electrostatic, and coupled fields, on the inner flow of the droplet are predicted, respectively, to reveal the evaporation differences caused by the electrostatic force.

Numerical model and mathematical formulations

Model description

Figure 1 illustrates a two-dimensional (2D) axisymmetric computational model for the problems to be studied here. A hemispherical water droplet of radius R , density $\rho_l = 998 \text{ kg/m}^3$, viscosity $\mu_l = 0.001 \text{ Pa s}$, relative permittivity $\epsilon_l = 81$, and conductivity $\sigma_l = 5 \times 10^{-4} \text{ S/m}$ is put on the insulating plate. The above plate with a separation distance of $8R$ is set as the heat source to heat the fluid. The parallel plates consist of a capacitor to apply a steady and uniform electrostatic field (the base plate is connected to high potential and the upper one is grounded). To discharge the conducted gas by evaporation process, the left and right profiles are set as outlet boundary conditions.

Table I. Surface tension coefficient of water.

Temperature (K)	273	283	293	303	313	333	353	373
STC (N/m)	0.0756	0.0742	0.0728	0.0712	0.0696	0.0662	0.0626	0.0589

STC: surface tension coefficient.

y represents surface tension coefficient and x is the temperature.

Governing equations

For a multi-field-phase mass transfer problem, we assume the fluids are immiscible and incompressible. The governing equations include mass conservation and N-S equation

$$\nabla \cdot \mathbf{U} = 0 \quad (1)$$

$$\frac{\partial \rho U}{\partial t} + \nabla \rho U^2 = -\nabla p + \nabla \cdot [\mu(\nabla U + \nabla U^T)] + \mathbf{F}_E \quad (2)$$

where U is the velocity, ρ is the density, p is the pressure, μ is the viscosity, q^v is the volume charge density, ϵ_0 is the permittivity of vacuum, and ϵ is the relative dielectric constant of the fluid. \mathbf{E} is the electric field strength. \mathbf{F}_E is the electric body force and can be expressed as equation (3)

$$\mathbf{F}_E = q^v \mathbf{E} - \frac{1}{2} \mathbf{E}^2 \nabla \epsilon + \nabla \left(\frac{1}{2} \mathbf{E}^2 \frac{\partial \epsilon}{\partial \rho} \rho \right) \quad (3)$$

The third term on the right as electrostriction is ignored since it has no influence on the hydrostatics as the mass density in the liquid remains constant.

Consider that the surface tension significantly influences the inner flow of the droplet; the surface tension coefficient (STC) is solved as a linear function with the temperature as shown in equation (4). The linear result is based on Table 1

$$y = 0.12179 - 1.6769 \times 10^{-4} x \quad (4)$$

A leaky dielectric model is used here to calculate the electric field distribution. This model must satisfy that the electric relaxation time of the fluid is much less than its viscous time, $t^E \ll t^v$, $t^E = \epsilon/\sigma$, and $t^v = \rho L^2/\mu$, where L is the characteristic length of the fluid. Namely, this assumption thinks that the free charges q^v in the fluid move to equilibrium almost instantly. Therefore, equation (5) can be simplified as equation (6). The advantage of this theory is that the free charges' resident property in the fluid evolution process is neglect, which greatly simplifies the complex charging process

$$\frac{Dq^v}{Dt} = \frac{\partial q^v}{\partial t} + \mathbf{U} \cdot \nabla q^v = -\nabla \cdot (\sigma \mathbf{E}) \quad (5)$$

$$0 = \nabla \cdot (\sigma \mathbf{E}) \quad (6)$$

In the liquid-gas multiphase flow system, the liquid phase easily satisfies the above assumption, but it is not suitable for the gas phase. Consider that the physical behaviors inside the evaporating droplet are the most concerns the electric body force is calculated only on the liquid phase as well as the interface. If the electric body force acts on the gas phase, some unexpected perturbations will happen. This is because in reality, the free charges' diffusion in the gas flow is much slow. Before they reach the distribution equilibrium, the local gas is already moves pass. Approximately, the electric body force is neglect in the gas phase, but the electrostatic field is calculated in the entire computational region to get a continuous field distribution.

The electric field intensity \mathbf{E} in equation (6) can be calculated as

$$\mathbf{E} = -\nabla \phi \quad (7)$$

Substituting this equation into equation (6), the electrostatic field formula can be expressed as

$$\nabla \cdot (\sigma \nabla \phi) = 0 \quad (8)$$

The electrostatic field distribution can be obtained from equation (8), and then the electric field intensity \mathbf{E} will be calculated. The volume charge density can be obtained through equation (9)

$$q^v = \nabla \cdot (\epsilon \mathbf{E}) \quad (9)$$

By solving the above parameters, the electric body force for constant density fluid system can be obtained by equation (10)

$$\mathbf{F}_E = -\frac{1}{2} \mathbf{E} \cdot E \nabla \epsilon + q^v \mathbf{E} \quad (10)$$

The heat flow equation is solved as

$$\rho c_p \frac{DT}{Dt} = \nabla(k \nabla T) + \frac{Dp}{Dt} + S_{evap} \quad (11)$$

where T is the temperature, c_p is the specific heat capacity, k is the thermal conductivity, and S_{evap} is the source term.

The mass transfer of the fluid is determined by the following equation

$$m = C \cdot \alpha \rho_l \frac{(T - T_{sat})}{T_{sat}} \quad (12)$$

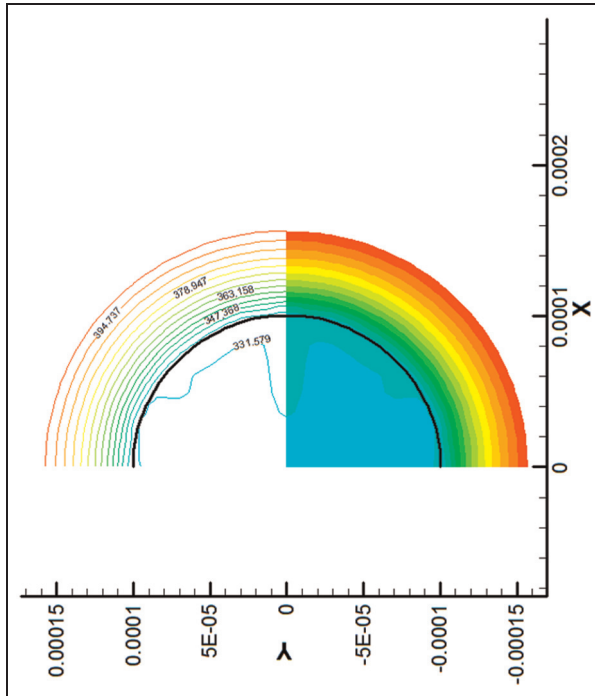


Figure 2. Evaporation isotherms at 20 ms in 500 K high-temperature field.

where C is an experienced parameter and the value is 0.1.¹⁴ To simplify the evaporation process, the product produced by the water evaporation is considered as air rather than vapor in this simulation, which can avoid calculating the mass, energy, and charge diffuse by accounting the variation in the fluid properties.

Then the source term S_{evap} can be expressed as

$$S_{evap} = -m \cdot L_{LHV} \quad (13)$$

The minus on the right side of the equation means evaporation is an endothermic process.

To capture the free interface of the droplet and ambient air, a VOF method is used in this article. The volume fraction α in the VOF method is defined as equation (14). The physical parameters are linear interpolated on the interface such as equation (15)

$$\alpha = \frac{V_l}{V} \quad (14)$$

where V_l is the liquid volume and V is the total volume

$$\left. \begin{aligned} \rho &= \alpha \rho_{liq} + (1 - \alpha) \rho_{gas} \\ \varepsilon &= \alpha \varepsilon_{liq} + (1 - \alpha) \varepsilon_{gas} \\ \sigma &= \alpha \sigma_{liq} + (1 - \alpha) \sigma_{gas} \end{aligned} \right\} \quad (15)$$

Results and discussion

A water droplet with 0.1 mm radius, 90° contact angle, and $T = 303$ K is suddenly put on to the base plate.

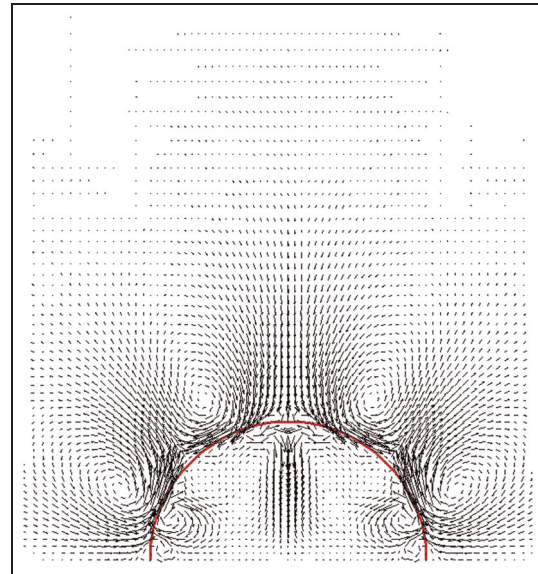


Figure 3. Evaporation flow field at 20 ms in 500 K high-temperature field.

The ambient air temperature is 500 K and the thermal radiation is not considered. First, due to the temperature gradient, the heat is transported through the interface into the droplet which makes its temperature to rise up. Instantly, the surface of the droplet is heated over the boiling point (373 K), and then the evaporation begins. The latent heat of vaporization in turn reduces the ambient temperature as shown in Figure 2. The temperature gradient-induced Marangoni stresses and velocity flow drag the fluid from warm regions, small surface tension areas, to the cold regions, larger surface tension areas, which lead to the circulation flow patterns as shown in Figure 3. The continuous brisk temperatures promote the droplet unstable. The stationary of the liquid near the original point (seen in Figure 4) causes the appearance of the bubble as shown in Figure 5.

After applying different electric potentials on the plates, a parallel-plate electrostatic system (Figure 1) is formed to influence the droplet. The result is shown in Figure 6. The velocities along the axis at different times of the droplet in the electrostatic field are predicted in Figure 7. The figure shows that the flow inside the charged droplet is stable except the regions near the interface. The electric body force drags the droplet slightly oblate.

It is interesting to note that the flow pattern and direction inside the evaporating droplet in Figure 3 are similar to the one which is affected by the single electrostatic field in Figure 6. It is concerned whether the electrostatic field effect could enhance the evaporation process of the droplet under high temperature. Under the proposal, the coupled electrostatic field evaporation model is practiced. The flow velocities along the axis

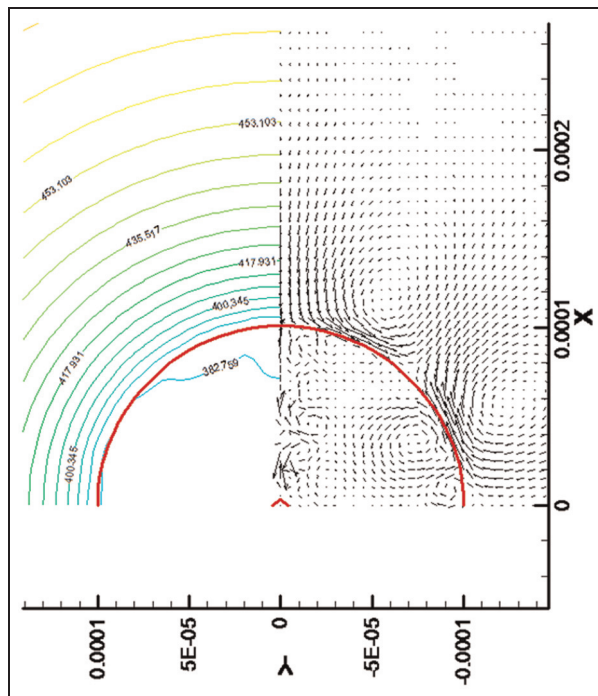


Figure 4. Flow velocity along the axis at 66.9 ms in electrostatic field.

under different acting fields are obtained in Figure 8. It can be found that the velocity in the coupled fields is lower than the other two. That means the electrostatic field slows the flow inside the droplet. To understand

this particular result, a deep analysis of the flow field of the liquid in each acting condition is needed.

The velocity vector distributions in the droplet under different affecting fields are displayed in Figure 9. Figure 9(a) illustrates the time dependence of the flow pattern as evaporation takes place under high-temperature field. In the initial stage, the large temperature gradient on the interface induces the variation and nonuniform distribution of the droplet surface tension which drags the liquid flow disordered shown in 40 and 50 ms. As the heat transfers into the droplet, the variation in the surface tension on the interface becomes less obvious. The vortexes inside the droplet merge gradually at 60 ms.

When the evaporation processes are affected by the electrostatic field, the streamlines of the liquid keep a steady state as shown in Figure 9(b). The velocity distribution along the axis is shown in Figure 10(b). The electric body force overcomes the forces induced by temperature gradient and drives the liquid moving in a circular pattern. The electrostatic field curbs the generation of extra vortexes compared with (a) and (b) in Figure 9 which leads to a reduction in the electric body force. Therefore, the driven flow is slower than that in single high-temperature or electrostatic field shown in Figure 8. This momentum loss process is similar to the coalescence of vortexes in Figure 9(a) under high-temperature field, the axis velocity distribution of which is displayed in Figure 10(a). At 0.05 s (the eve of the coalescence), the velocity along the axis is the lowest one.

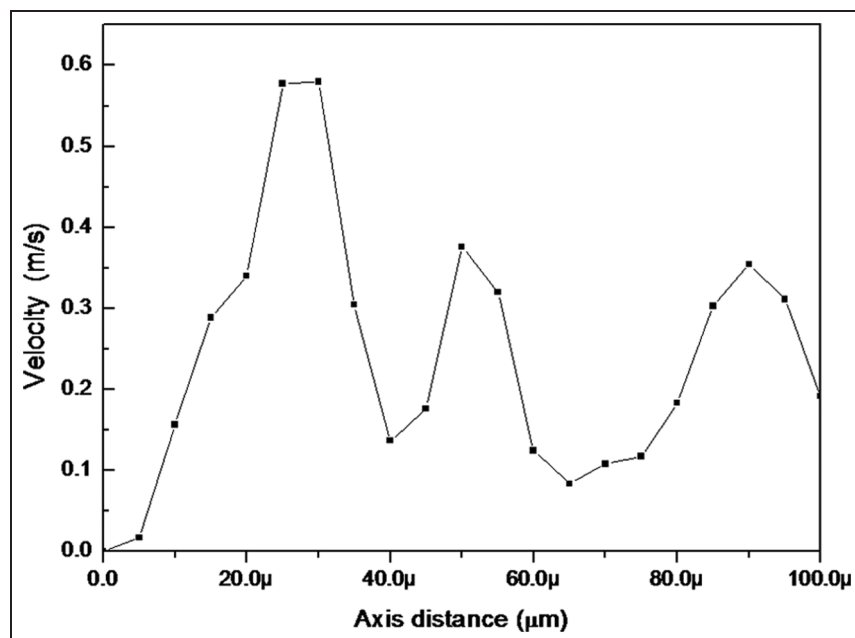


Figure 5. Bubble appears at 66.9 ms in 500 K high-temperature field.

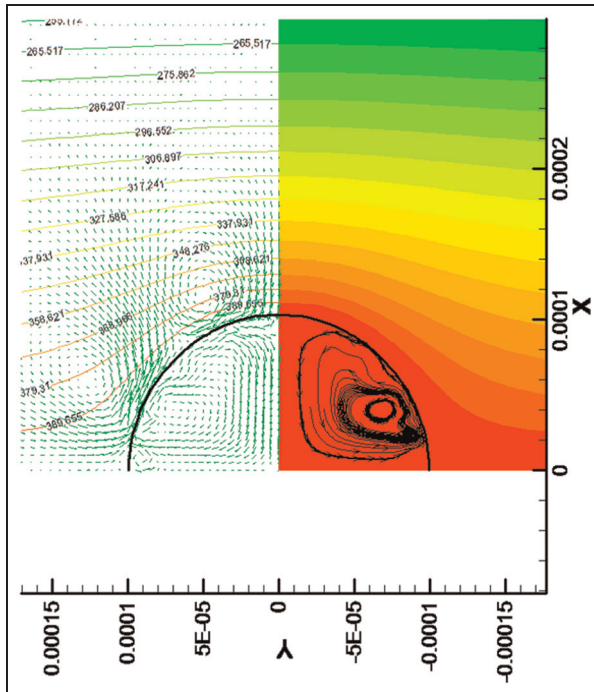


Figure 6. Inner flow pattern of the charged droplet in electrostatic field (E is 500 kV/m).

If the electric potential applied on the base plate is not high enough, more vortexes will exist inside the droplet as shown in Figure 11. In Figure 11(b), two major vortexes in the droplet at $E = 20, 50$, and 100 kV/m, respectively. The electric body force is less strong to totally negate the effects of the forces caused

by temperature gradient under these electric intensities. Therefore, more than one large vortex is induced. Despite the low electric intensity in Figure 11(a), the flow field keeps constant. The stable property of the electrostatic field makes it to continuously restrict the flow of the liquid phase as shown in Figure 12(a). The velocity distribution along the axis in different electric potentials is displayed in Figure 12(b). It is confirmed that higher the electric intensity, faster the circle flow velocity inside the droplet. But the velocity distribution trends along the axis are different. The velocity under lower electric field intensity (20, 50, and 100 kV/m) is continually raised while under the higher field intensity condition (500 kV/m) is decreased first and then increased. The vortex effect is directly determined by the distance from fluid location to the vortex center. The closer the point to vortex center, the faster the fluid moves. In lower electric field intensity, the points along the axis are affected by two main vortexes. From the original point to the equator, the distance of the points along the axis to the lower vortex center is first near and then far, but the higher vortex works as a relay station to keep the velocity increasing. In higher electric field intensity condition, the flow behavior is simpler; one main vortex makes the velocity distribute like a normal distribution.

Comparing (a) and (b) in Figure 10, it can be clearly found that the maximum velocity in high-temperature field (about 0.4 m/s) is much larger than that in the coupled fields (about 0.075 m/s). This leads to a significant difference of transportation of heat from gas phase to the droplet as shown in Figure 13. The increase in

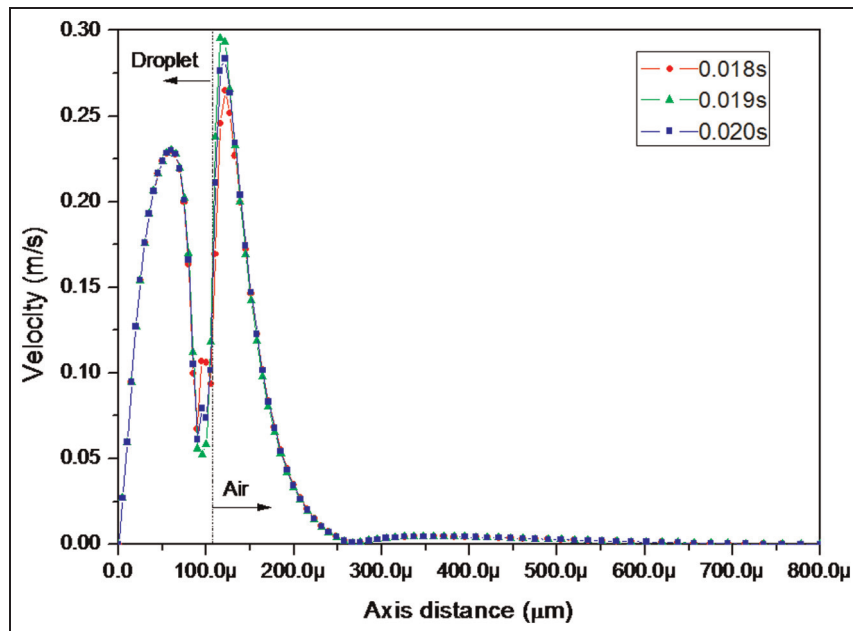


Figure 7. Flow velocity along the axis in electrostatic field (E is 500 kV/m).

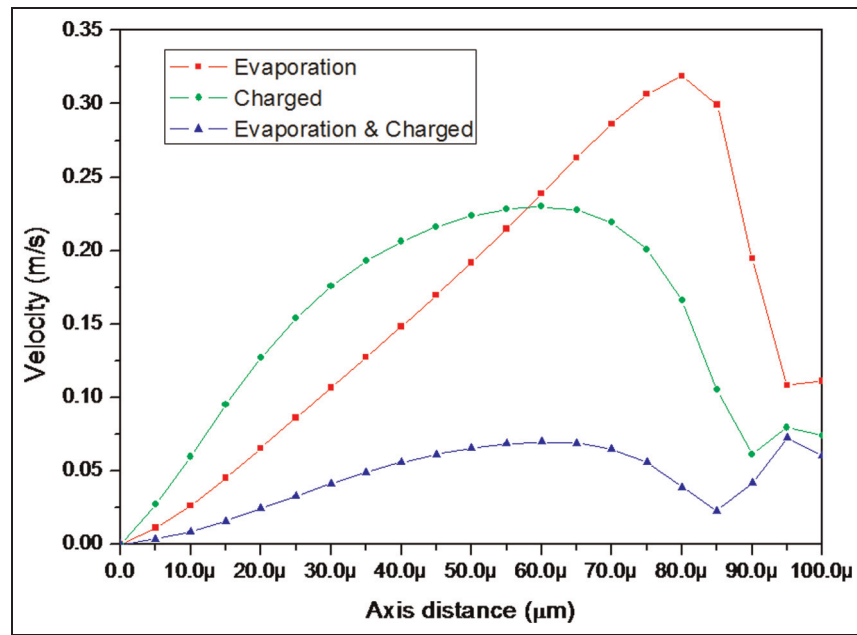


Figure 8. Flow velocity along the axis (the time is 20 ms; in charged case, E is 500 kV/m).

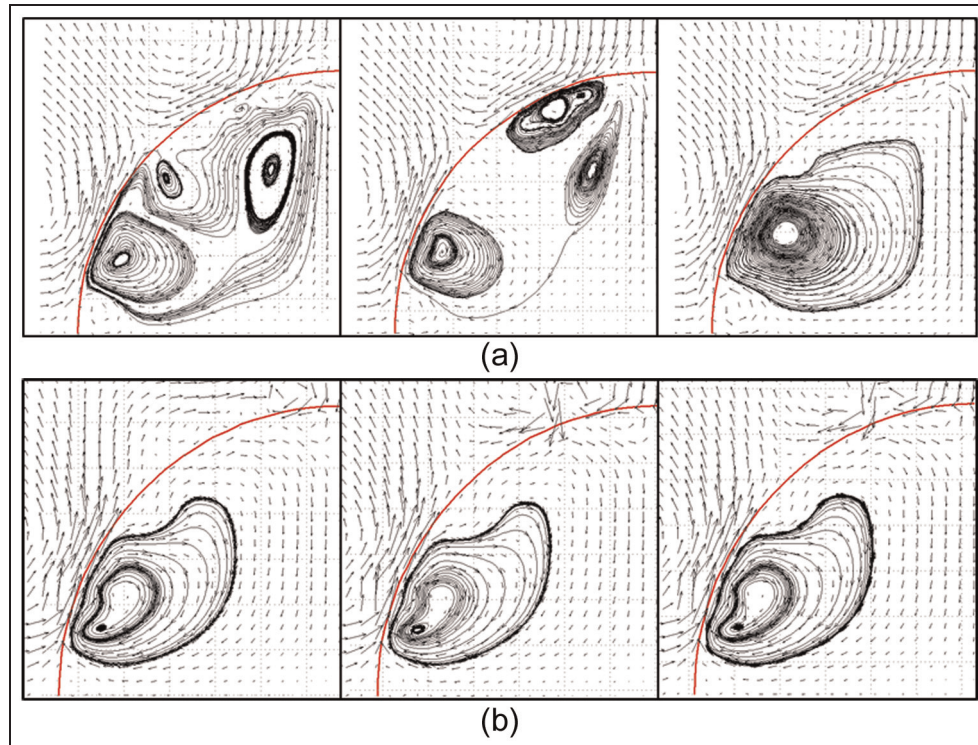


Figure 9. The inner flow pattern of the droplet: (a) droplet in the high-temperature field at time 40, 50, and 60 ms and (b) droplet in the coupled high temperature at time 10, 40, and 60 ms; the electrostatic field intensity is 500 kV/m.

temperature on the original point inside the droplet under the coupled fields is more slowly which leads to a lower evaporation rate of the droplet as displayed in

Figure 14. Due to the appearance of the bubble, the curve of the evaporated droplet in high-temperature field is not linear.

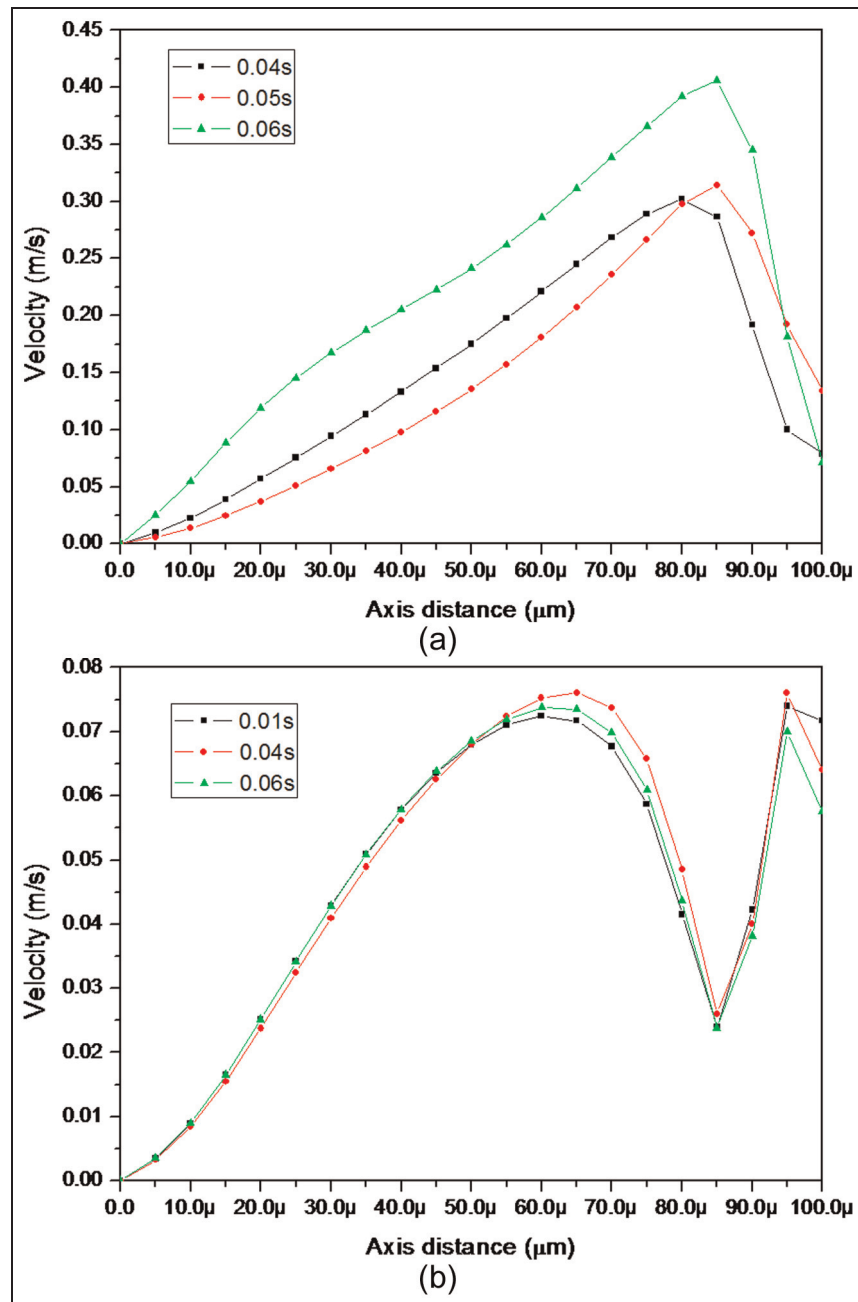


Figure 10. Inner flow velocity rate along the axis of the droplet: (a) droplet in single temperature field and (b) droplet in coupled fields; the electric field intensity is 500 kV/m.

Conclusion

The evaporation of a sessile droplet under high-temperature and coupled electrostatic field is simulated. In high-temperature field, the large temperature gradient on the interface at the initial stage induces lots of vortexes inside the heated droplet. The vortexes enhance the heat transfer from ambient air to the droplet. The external electrostatic field restrains the flow

inside the droplet and keeps a steady circulation. The flow velocity is reduced due to the interaction between electric body force and the force caused by temperature gradient. Lower flow velocity reduces the heat transfer into the droplet. The evaporation rate of the droplet in the high-temperature field is declined. This means the droplet can exist for a longer time in high-temperature condition by the effect of the electrostatic field. It may be useful in dust control for high-temperature flue gas.

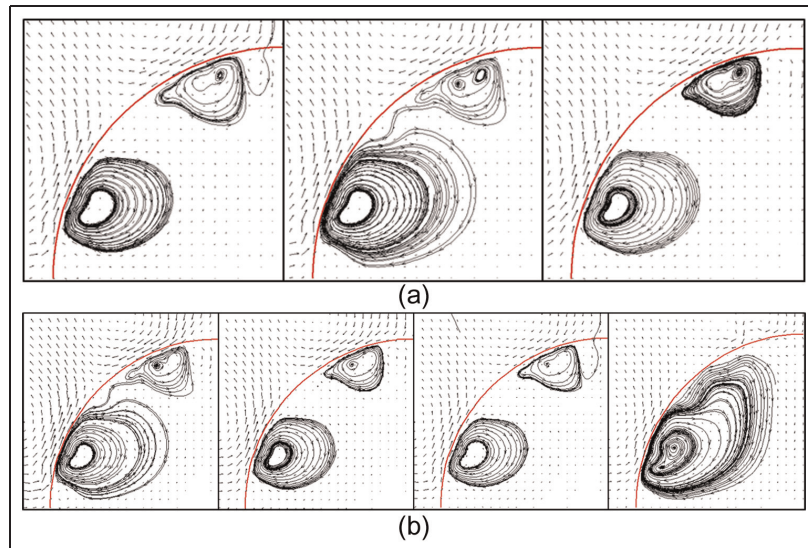


Figure 11. Inner flow pattern of the droplet with different electric field intensities and times: (a) E is 20 kV/m; times are 10, 40, and 60 ms and (b) time is 70 ms; E is 20, 50, 100, and 500 kV/m.

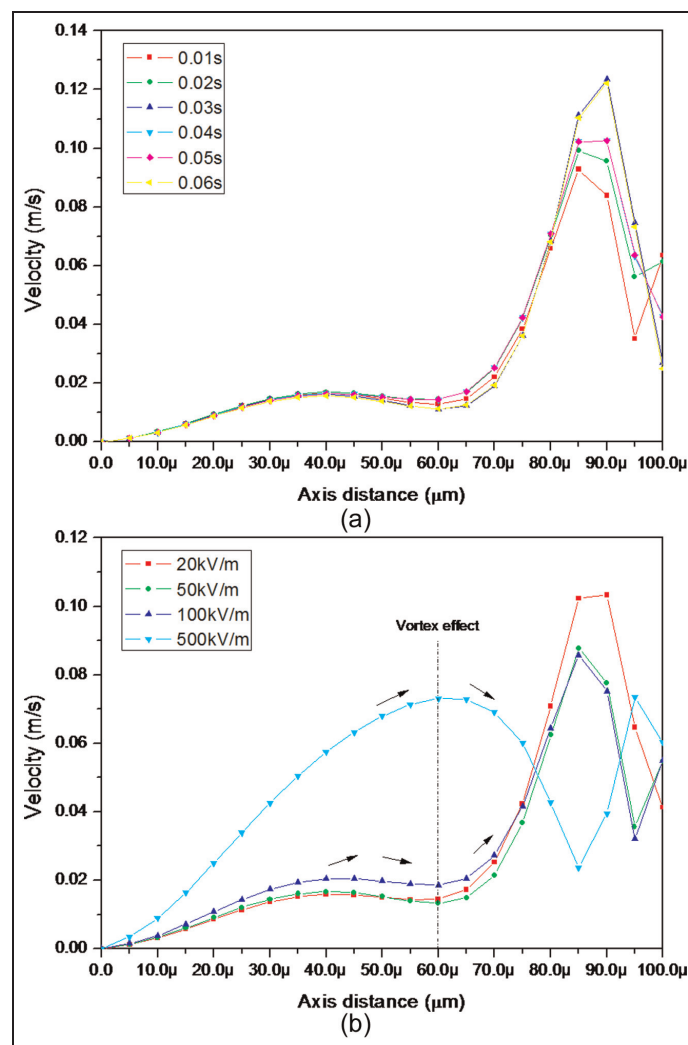


Figure 12. The inner axis flow velocity rate of the charged droplet under coupled fields: (a) The electric intensity is 20 kV/m and (b) all cases with the same time at 70 ms.

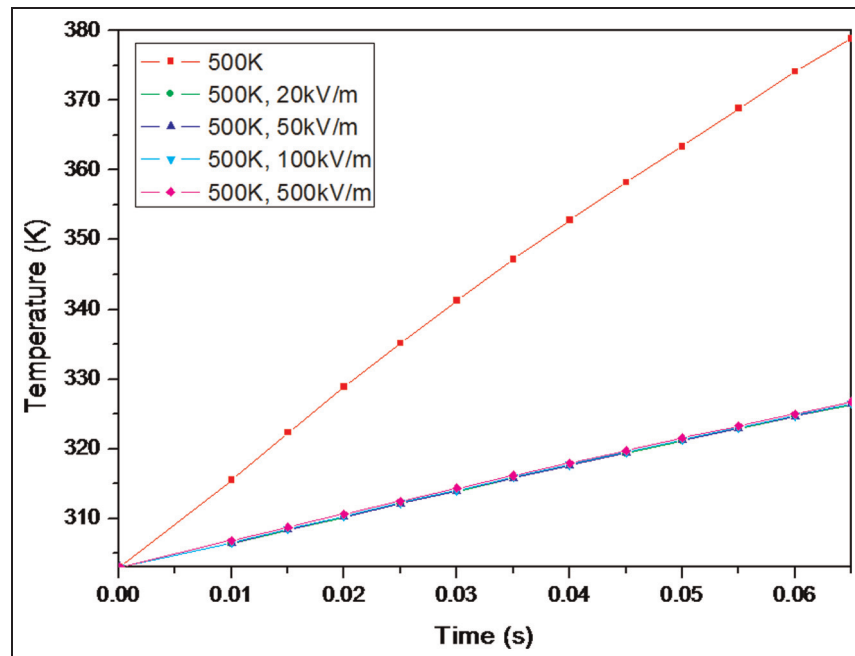


Figure 13. Temperature distribution (original point).

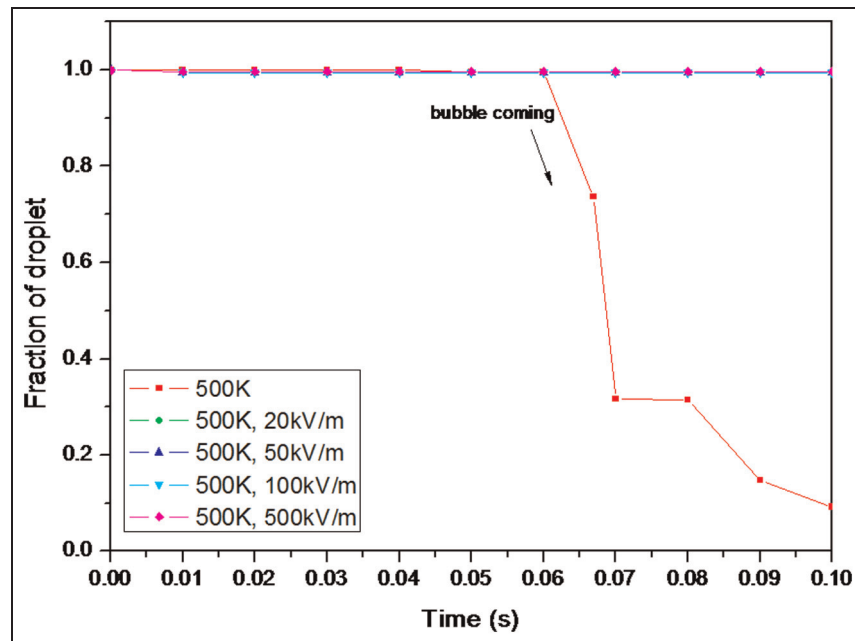


Figure 14. Evaporation rate of the droplet.

Declaration of conflicting interests

The authors have declared that no conflict of interest exists.

Funding

The authors thank the support from Natural Science Foundation of China (NSFC) (No. 51106064 and No.

51376084) and Postgraduate scientific research and innovation project of Jiangsu (PSRIPJ) (No. KYLX_1037).

References

- Renksizbulut M and Yuen MC. Experimental study of droplet evaporation in a high-temperature air stream. *J Heat Tran* 1983; 105(2): 384–388.

2. Renksizbulut M and Yuen MC. Numerical study of droplet evaporation in a high-temperature stream. *J Heat Tran* 1983; 105(2): 389–397.
3. Harpole GM. Droplet evaporation in high temperature environments. *J Heat Tran* 1981; 103(1): 86–91.
4. Abramzon B and Sirignano WA. Droplet vaporization model for spray combustion calculations. *Int J Heat Mass Tran* 1989; 32(9): 1605–1618.
5. Tseng CC and Viskanta R. Effect of radiation absorption on fuel droplet evaporation. *Combust Sci Technol* 2005; 177(8): 1511–1542.
6. Hashinaga F, Kharel GP and Shintani R. Effect of ordinary frequency high electric fields on evaporation and drying. *Food Sci Technol Int* 1995; 1(2): 77–81.
7. Gamero-Castano M. Electric-field-induced ion evaporation from dielectric liquid. *Phys Rev Lett* 2002; 89(14): 147602.
8. Balachandran W, Jaworek A, Krupa A, et al. Efficiency of smoke removal by charged water droplets. *J Electrostat* 2003; 58(3): 209–220.
9. Bateni A, Amirfazli A and Neumann AW. Effects of an electric field on the surface tension of conducting drops. *Colloid Surface Physicochem Eng Aspect* 2006; 289(1): 25–38.
10. Chen L, Li C, Van der Vegt NFA, et al. Initial electro-spreading of aqueous electrolyte drops. *Phys Rev Lett* 2013; 110(2): 026103.
11. Vancauwenberghe V, Di Marco P and Brutin D. Wetting and evaporation of a sessile drop under an external electrical field: a review. *Colloid Surface Physicochem Eng Aspect* 2013; 432: 50–56.
12. Taylor G. Studies in electrohydrodynamics. I. The circulation produced in a drop by electrical field. *Proc Math Phys Eng Sci* 1966; 291(1425): 159–166.
13. Hirt CW and Nichols BD. Volume of fluid (VOF) method for the dynamics of free boundaries. *J Comput Phys* 1981; 39(1): 201–225.
14. Lee WH. Pressure iteration scheme for two-phase flow modeling. In: Nejat Veziroglu T (ed.) *Multiphase transport: fundamentals, reactor safety, applications*. Washington, DC: Hemisphere Publishing Corporation, 1980, pp.407–432.